# Does Higher Datarate Perform Better in IEEE 802.11-based Multihop Ad Hoc Networks?

Frank Y. Li, Andreas Hafslund, Mariann Hauge, Paal Engelstad, Øivind Kure, and Pål Spilling

*Abstract:* **Due to the nature that high datarate leads to shorter transmission range, the performance enhancement by high datarate 802.11 WLANs may be degraded when applying high datarate to an 802.11 based *multihop* ad hoc network. In this paper, we evaluate, through extensive simulations, the performance of multihop ad hoc networks at multiple transmission datarates, in terms of the number of hops between source and destination, throughput, end-to-end delay and packet loss. The study is conducted based on both stationary chain topology and mesh topologies with or without node mobility. From numerical results on network performance based on chain topology, we conclude that there is almost no benefit by applying the highest datarate when the chain length is 6 hops or more. With node mobility in mesh topology, the benefit of using high datarate diminishes at even shorter number of hops. To explore the main reasons for this behavior, analyses on multihop end-to-end throughput and network $k$-connectivity have been conducted later in the paper, and correspondingly an auto-rate adaptation algorithm has been proposed.**

*Index Terms:* **Ad hoc networks, IEEE 802.11b/g, multihop, multirate, network connectivity, performance simulation and analysis, rate adaptation algorithm.**

## I. INTRODUCTION

The IEEE 802.11 specification on medium access control (MAC) and physical (PHY) layers has been used as the *de facto* standard for ad hoc networking. In addition to the original basic daterates of 1 and 2 Mbps [1], the enhanced standards offer also much higher raw daterates of up to 11 Mbps for 802.11b [2], and 54 Mbps for 802.11g [3] and 802.11a. Products with even higher datarates are expected to appear soon as the 802.11n standard [4] has been ratified by the dot11n task group in March 2007. However, the 802.11 standard is primarily targeted at single hop wireless local area networks (WLANs), and the high datarate is achieved at a price of shorter transmission range, given the same channel condition [5].

To select a suitable datarate in a WLAN, one may perform either the sender-based algorithm that relies on counting the number of acknowledgment received at the sender [6], or the receiver-based algorithm which adjusts the datarate based on received signal strength [7]. Whatever method to apply, the objective for rate adaptation in WLANs is quite straightforward: identify the highest possible datarate, for achieving highest throughput and shortest delay.

In *multihop* ad hoc networks, however, adopting high datarate is somewhat paradoxical. On the one hand, transmitting at higher datarate may achieve higher one-hop throughput and shorter per-hop delay. On the other hand, adopting higher datarate may also lead to more hops from source to destination and weaker network connectivity, which in return may result in a throughput and delay degradation. This dilemma motivates our study on the performance of multiple datarates in multihop ad hoc networks in this paper.

Given the fact that a high datarate provides better performance in terms of throughput and delay in one-hop WLANs, we are trying to answer the following questions in this paper:

- Can higher datarates also achieve better performance over lower datarates in *multihop* wireless networks? If yes, in which circumstances?
- Given multiple available datarates, how can we select the best datarate for achieving highest possible end-to-end throughput in a *multihop* wireless network?

To answer these questions, we first review the 802.11 MAC and PHY layers briefly, and then draw a few observations which form the basis for this study. Based on scenarios built on both chain topology and mesh topology with and without node mobility, we conduct extensive simulations afterwards. One major result of this paper is that we have demonstrated, using numerical values, that high datarates may not perform better than lower datarates in *multihop* ad hoc networks, in terms of such parameters as the number of hops, achieved throughout at the destination node, packet loss and end-to-end (ETE) delay. Longer path length and less network connectivity are two main reasons for this performance degradation at high datarate. By using connectivity as a criterion for rate selection, an automatic rate adaptation algorithm has been proposed later in the paper.

The rest of this paper is organized as follows. The background information and observations are discussed in Section II, and afterwards the simulation configuration is explained in Section III. Sections IV and V present our simulation work using 802.11b regarding a static chain topology and a mesh topology with node mobility, respectively. Furthermore, Section VI presents instead another set of simulations based on a static network with uniform node distribution, using 802.11g. Later on, the analytical work is presented in Section VII, together with a proposed rate adaptation algorithm. Moreover, some related work is outlined in Section VIII before the conclusions are drawn in Section IX.

Manuscript received August 18, 2004, approved for publication by Mario Gerla, Division III editor, August 22, 2007.

F. Y. Li is with the Department of Information and Communication Technology, University of Agder, Grimstad, Norway, email: frank.li@uia.no.

A. Hafslund is with Telenor Networks, Fornebu, Norway, email: andreas.hafslund@telenor.com.

M. Hauge is with the Norwegian Defense Research Establishment (FFI), Kjeller, Norway, email: mariann.hauge@ffi.no.

P. Engelstad is with Telenor R&I, Fornebu, Norway, email: paal.engelstad @telenor.com.

Ø. Kure is with the Department of Telematics, Norwegian University of Science and Technology (NTNU), Trondheim, Norway, email: okure@item. ntnu.no.

P. Spilling is with UniK - University Graduate Center, University of Oslo, Kjeller, Norway, email:paal@unik.no.

1229-2370/07/$10.00 

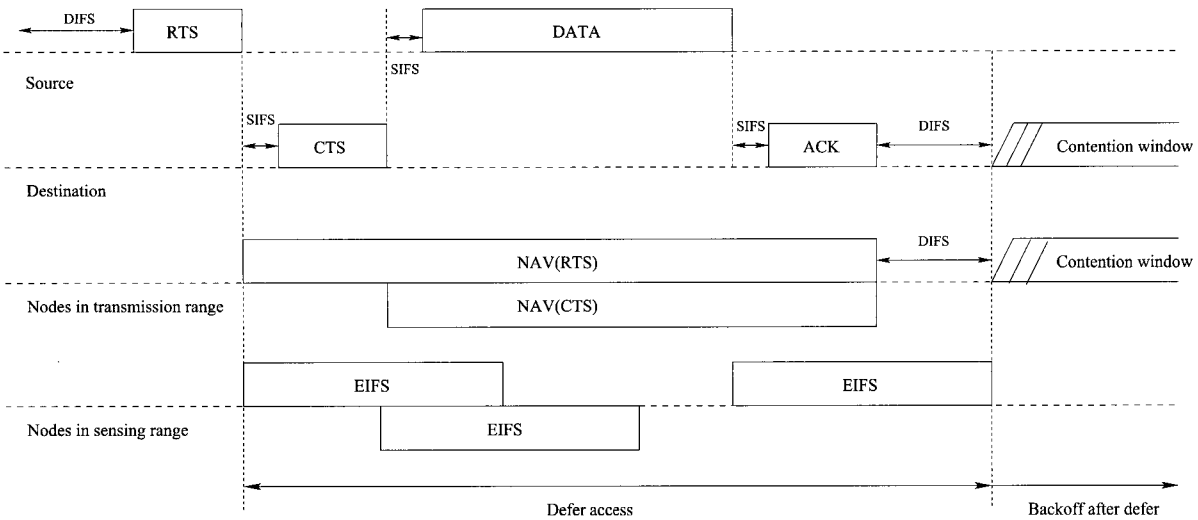


Fig. 1. NAV and EIFS [8].

## II. BACKGROUND INFORMATION AND OBSERVATIONS

In this section, we provide some in-depth background information on MAC and PHY layers in the 802.11 standard which are relevant to this study. Based on the description, we later outline a few useful observations.

### A. Brief Description of the DCF in 802.11

There exists two channel access mechanisms for distributed coordination function (DCF) in the 802.11 MAC specification. That is, the basic carrier sense multiple access with collision avoidance (CSMA/CA) mechanism and the additional request to send/clear to send (RTS/CTS) mechanism. Throughout the context, the abbreviation CSMA/CA or RTS/CTS refers to CSMA/CA without RTS/CTS or CSMA/CA with RTS/CTS, respectively.

Fig. 1 illustrates the principle of the MAC mechanism in 802.11, which shows how a station within different ranges updates its backoff interval respectively by network allocation vector (NAV) or extended inter frame space (EIFS), depending on whether it can correctly decode the *duration* field in the MAC header or not. Refer to [1] for more detailed description.

### B. PHY Frame Structure and Transmission Datarate in 802.11

Both mandatory long physical layer convergence protocol (PLCP) preamble and optional short preamble frame are defined in the physical frame format of 802.11. As an example, the long PLCP preamble in 802.11b is depicted in Fig. 2.

As we can easily observe from Fig. 2, when 802.11b is used, the PLCP header is always transmitted at 1 Mbps, while the MPDU may be transmitted at 2, 5.5, or 11 Mbps. *As the PLCP header is always appended to any MPDU fragment, it means that one of the basic datarates always exists as part of any frame transmission in 802.11, albeit whatever datarate the MPDU is using.* For instance in 802.11b, when a MAC frame is transmitted at the highest datarate 11 Mbps, part of the frame is still transmitted at 1 Mbps. That is, for any types of frames, only

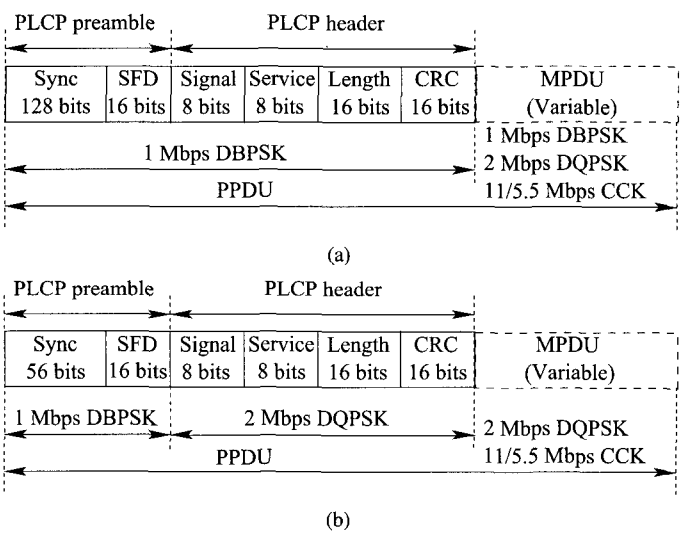


Fig. 2. Frame structures of the physical layer in 802.11b: (a) Long preamble, (b) short preamble.

the MPDU part is transmitted at a higher datarate. Furthermore, to support the proper operation of the RTS/CTS and the virtual carrier sense mechanism, the whole RTS and CTS frames shall be transmitted at one of the basic datarates, e.g., 1 Mbps or 2 Mbps when 802.11b is used.

### C. Observation of Three Ranges

As well understood, the benefit of using higher datarates is achieved at a cost of stronger requirement for signal-to-interference-and-noise ratio (SINR), for achieving the same bit error rate (BER), resulting in shorter transmission range.

Keeping this fact in mind and looking at the physical frame format once again in Fig. 2, we can easily observe that *there always exist three ranges* [1] *in any frame transmission in 802.11.* That is, $R_{tx}^{L}$ for low datarate, $R_{tx}^{H}$ for high datarate where

[1] Only two ranges for datarates 1 Mbps in 802.11b and 6 Mbps in 802.11g.

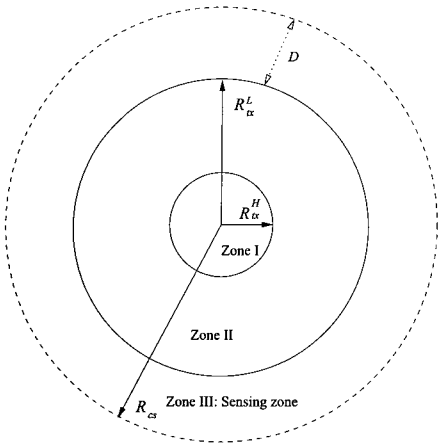


Fig. 3. Observation of three ranges in 802.11 networks. $R_{tx}^L$ denotes the transmission range for low data rate, $R_{tx}^H$ denotes the transmission range for high data rate, and $R_{cs}$ denotes the carrier sensing range. (Zone I: area covered by $R_{tx}^H$; Zone II: area covered by $R_{tx}^L$; Zone III: area covered by $R_{cs}$ excluding Zone II).

$R_{tx}^L > R_{tx}^H$, and the sensing range $R_{cs}$. The sensing range defines an area where any node within $R_{cs}$ will determine the medium as busy, while a node in the mid of the circle is transmitting. Fig. 3 illustrates our observation of these three ranges. The interference range, which is not shown in this figure, depends on the distance between the inferencing node and the receiver, as well as SINR. More discussions on the interference range can be found later in Section VII.

It is quite straightforward to refer to $R_{tx}^L$ as the transmission range for RTS/CTS frames and $R_{tx}^H$ as the transmission range for DATA frame when RTS/CTS is enabled. With the basic CSMA/CA mechanism, $R_{tx}^L$ corresponds to the larger transmission range for the PLCP header, while $R_{tx}^H$ is the transmission range for the MPDU part of a DATA frame. In this case, nodes within Zone II but beyond Zone I can only defer a fixed interval of EIFS.

Another observation here is that the sensing range $R_{cs}$, with $R_{cs} = R_{tx}^L + D$ in Fig. 3, is the same for all transmission datarates, for identical transmission power. As a consequence, the ratio between the sensing range and the DATA transmission range is larger for higher datarate. Studies on how to optimally define the sensing range can be found, e.g., in [9]–[12].

### D. Theoretical Throughput and MAC Delay in 802.11

The theoretical maximum throughput (TMT) and theoretical one-hop delay can be calculated for various 802.11 implementations. Table 1 lists a few concrete values [13] used in this paper by assuming a direct sequence spread spectrum (DSSS) or orthogonal frequency division multiplexing (OFDM) physical layer implementation, where TMT and delay denote the TMT and the average one-hop delay when channel is idle, for given MPDU length. These values are listed here as a reference when we later compare the performance of the multihop ad hoc networks versus one-hop WLANs.

**Summary of this section**: By discussing a few relevant MAC and PHY layer issues in 802.11, we have made the following observations, which constitute the basis for our further study in this paper.

- Higher datarate leads to shorter transmission range. This means that more hops may be needed between source and destination in multihop ad hoc networks at higher datarates.
- At any datarate, the physical header PLCP is always transmitted at the lowest datarate. Depending on whether the MAC frame being correctly decoded or not, a node within the sensing range defers by a NAV or an EIFS interval.
- There always exist *three ranges* for any frame transmission in 802.11; and the sensing range is identical for all datarates with constant transmission power.
- The maximum throughput in 802.11 is meant for one-hop WLAN, and the theoretical average delay is achieved when the channel is sensed as idle.

Table 1. Energy consumption for encoding and decoding RS code.

| | Rate (Mbps) | MPDU (bytes) | TMT (Kbps) | Delay (ms) |
|---|---|---|---|---|
| CSMA/CA | 1 | 1500 | 913 | 13.138 |
| RTS/CTS | 1 | 1500 | 869 | 13.814 |
| CSMA/CA | 5.5 | 1500 | 3874 | 3.097 |
| RTS/CTS | 5.5 | 1500 | 3180 | 3.773 |
| CSMA/CA | 11 | 1500 | 6056 | 1.982 |
| RTS/CTS | 11 | 1500 | 4515 | 2.658 |
| CSMA/CA | 6 | 500 | 4494 | 0.890 |
| RTS/CTS | 6 | 500 | 3983 | 1.004 |
| CSMA/CA | 54 | 500 | 17092 | 0.234 |
| RTS/CTS | 54 | 500 | 13337 | 0.300 |

Table 2. Transmission ranges at multiple datarates in 802.11b.

| | 11 Mbps | 5.5 Mbps | 2 Mbps | 1 Mbps |
|---|---|---|---|---|
| Outdoor | 160 m | 270 m | 400 m | 550 m |
| Semi-open | 50 m | 70 m | 90 m | 115 m |
| Indoor | 25 m | 35 m | 40 m | 50 m |
| Receiver sensitivity | −82 dBm | −87 dBm | −91 dBm | −94 dBm |

## III. SIMULATION CONFIGURATION

### A. Transmission Ranges

We use the transmission range values specified in Proxim ORiNOCO Classic Gold PC Card [14] as the basis for transmission range configuration in our simulation for 802.11b, as listed in Table 2. We use however specifications from another manufacturer for our simulation with 802.11g, as described in Section VI. Note that the values listed here are given by the card manufacturer, and transmission ranges in reality may vary considerably, depending on channel conditions and other factors [15]. However, how transmission range varies according to different channel conditions is beyond the scope of this study. We adopt, without losing generality, a simple channel model in our simulation, as presented in the next subsection.

Furthermore in our study, an outdoor environment is assumed

Table 3. Radio parameters used in 802.11b simulation.

| | |
|---|---|
| Antenna height | 1.5 m |
| Carrier frequency | 2452 MHz |
| Transmission power | 15 dBm |
| CPThreshold | 10 |
| CSThreshold | $9.5421 \times 10^{-13}$ ($R_{cs} = 640$ m ) |
| RXThreshold | $1.17 \times 10^{-10}$ (11 Mbps) |
| | $3.0123 \times 10^{-11}$ (5.5 Mbps) |
| | $6.2535 \times 10^{-12}$ (2 Mbps) |
| | $1.7495 \times 10^{-12}$ (1 Mbps) |

for all simulation scenarios. However, the simulation results for semi-open and indoor environment can easily be obtained by adjusting range parameters accordingly as listed in Table 2. Even though the concrete numerical values may vary correspondingly for those environments, we claim that the conclusions we draw later in the paper apply to all environments.

### *B. Configuration in ns2*

We use the ns2 simulator with CMU Monarch wireless extension [16] for our simulation. The two-ray ground reflection model is used as the propagation model and omnidirectional antenna with unit gain is assumed for both transmitter and receiver. The radio parameters in 802.11b simulation configuration are listed in Table 3.

The transmission power is always set as 15 dBm in our simulation, and corresponding transmission ranges at different datarates are achieved by adjusting the receiving threshold (RXThreshold in ns2). Indeed, fixed transmission power is one of the fundamental assumptions in this study and energy consumption at each node at different datarates is not within the interest of this paper.

Furthermore, the three range observation presented earlier has been implemented in our ns2 codes. The sensing range is set as 640 m in our 802.11b simulations, leading to the ratios between $R_{cs}$ and $R_{tx}^{H}$ as 4, 2.37, 1.6, or 1.16 at 11, 5.5, 2, or 1 Mbps, respectively. All simulation results shown in this paper are obtained with a simulation time of 100 seconds. The queue in each node is a first in first out (FIFO) queue with tail drop, and the queue length is 50 packets. The ad hoc on demand distance vector (AODV) protocol [17] is chosen as the routing protocol for scenarios in Sections IV and V, and the optimized link state routing (OLSR) [18] is used for scenarios in Section VI, respectively. No priority is given to protocol packets.

Both constant bit rate (CBR)/user datagram protocol (UDP) and file transfer protocol (FTP)/transmission control protocol (TCP) traffic are considered in this study. More details on traffic generation can be found later in the paper.

### *C. Simulation Scenarios*

Four scenarios are considered in our study, where the first two are based on a chain topology with stationary nodes while the third and the fourth deal with nodes located in two dimensional areas, with or without mobility, respectively. The basic features of the considered scenarios are listed in Table 4. With chain topology, there is only one traffic flow in the network, initiating at node 0 and terminating at node 12 or node 6. Note that for both static and mobile scenarios, we consider that all nodes along a source-destination path are using the same datarate and the datarate does not change during simulation lifetime. This assumption is reasonable given the fact that the performance of 802.11 is greatly degraded if different datarates are used at the same time within the one-hop vicinity [19].

Table 4. Simulation scenarios: Two for static chain topology and two for nodes with or without mobility, respectively.

| | $d$ | 11 Mbps | 5.5 Mbps | 2 Mbps | 1 Mbps |
|---|---|---|---|---|---|
| Scen. I | 150 m | 12 hops | 12 hops | 6 hops | 4 hops |
| Scen. II | 125 m | 12 hops | 6 hops | 4 hops | 3 hops |
| Scen. III | 100 nodes with mobility in a $1200 \times 1200$ m$^2$ area | | | | |
| Scen. IV | 100 stationary nodes in a $800 \times 800$ m$^2$ area [20] | | | | |

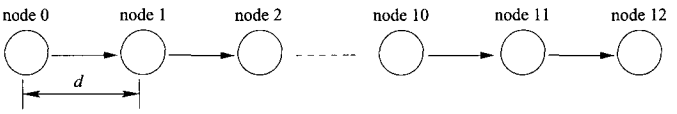


Fig. 4. 13 nodes in chain topology. The distances between any two neighboring nodes are identical and equal to $d$ meters. Only one source traffic flow from node 0 to node 12.

The chain topology is shown in Fig. 4. The distance between any two immediate neighboring nodes, denoted as $d$, is identical for all neighbor-pairs. Depending on the different transmission ranges listed in Table 2, the number of hops between source and destination varies at each datarate.

Scenario III in our study deals with multihop networks in a mesh topology with node mobility. 100 nodes are placed in a square area of $1200 \times 1200$ m$^2$. The stationary random waypoint model is employed as the mobility model in this study [21]. Two traffic patterns are generated in this scenario: 1) Homogeneous traffic, 4 CBR/UDP flows each at source bitrate 200 Kbps; 2) heterogeneous traffic, 4 FTP/TCP connections are generated, in addition to 4 CBR/UDP traffic flows. The TCP agent used is the base TCP sender (Tahoe TCP) with congestion control and round-trip-time estimation. The TCP packets are of length 1000 bytes, and the window size is set as 4. Among all nodes in the area, 8 or 16 nodes are arbitrarily chosen as the source and destination nodes, respectively in these two cases, and other nodes only act as relays when necessary.

Scenario IV focuses on performance of 802.11g based multihop networks with static uniform node distribution, where the relationship between datarate and network connectivity has been studied in depth.

## IV. NUMERICAL RESULTS FOR CHAIN TOPOLOGY

This section presents and discusses the simulation results we have obtained based on the scenarios for chain topology as described above.

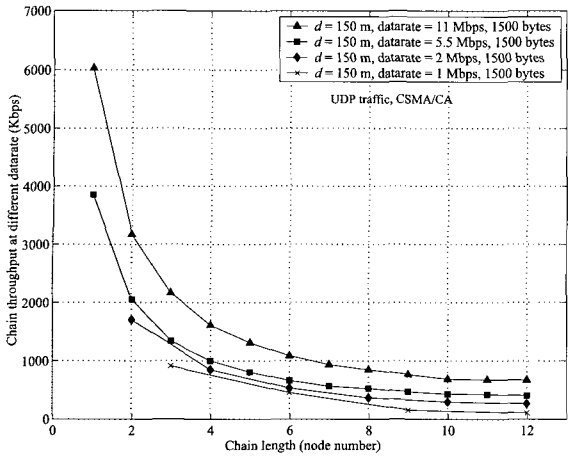


Fig. 5. Scenario I: maximum throughput for multihop ad hoc networks at different data rates. CBR/UDP traffic with CSMA/CA. The number of hops for data rate 11, 5.5, 2, or 1 Mbps is 12, 12, 6, or 4, respectively.

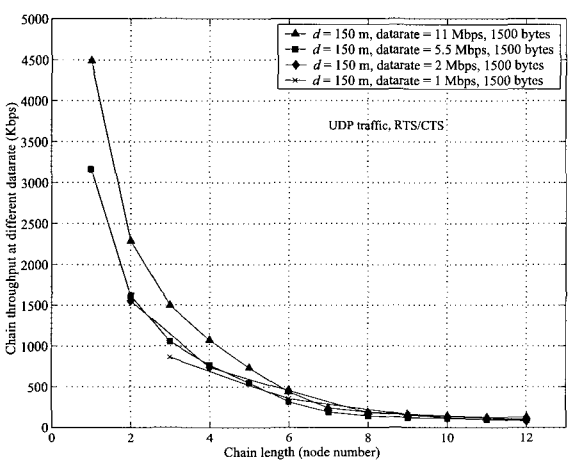


Fig. 6. Scenario I: maximum throughput for multihop ad hoc networks at different data rates. CBR/UDP traffic with RTS/CTS. The number of hops for data rate 11, 5.5, 2, or 1 Mbps is 12, 12, 6, or 4, respectively.

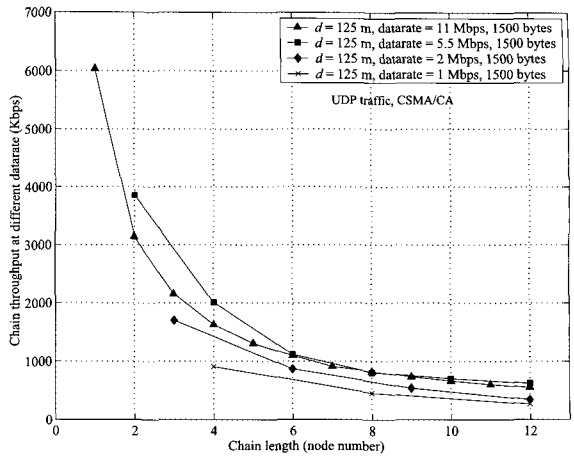


Fig. 7. Scenario II: maximum throughput for multihop ad hoc networks at different data rates. CBR/UDP traffic with CSMA/CA. The number of hops for data rate 11, 5.5, 2, or 1 Mbps is 12, 6, 4, or 3, respectively.

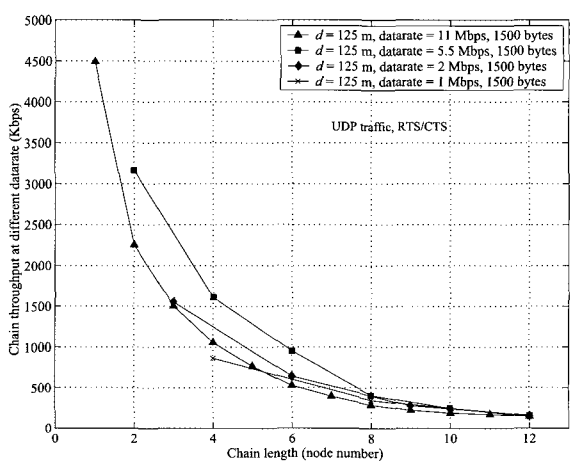


Fig. 8. Scenario II: maximum throughput for multihop ad hoc networks at different data rates. CBR/UDP traffic with RTS/CTS. The number of hops for data rate 11, 5.5, 2, or 1 Mbps is 12, 6, 4, or 3, respectively.

### A. *Maximum Chain Throughput at Multirates*

The authors in [22] concluded that the chain throughput in multihop ad hoc networks is $1/4 \sim 1/7$ of the maximum one-hop throughput (TMT), using the default ranges in ns2 as $R_{tx} = 250$ m and $R_{cs} = 550$ m. In this subsection, we investigate the maximum chain throughput at each datarate, based on our observations in Section II. A salient distinction between this study and the work in [22] is: The fact that lower datarate leads to shorter path, and vice versa, has been considered in this paper.

The purpose of this set of simulations is to find the *maximum* throughput in a multihop ad hoc network. So for all curves illustrated in Figs. 5–8, the traffic bitrate generated at the source node is slightly higher than the corresponding one-hop TMTs listed in Table 1. By doing so, there are always packets ready for transmission at the source node. In other words, the throughput simulated in these figures is the *saturation throughput for multihop networks*.[2] Another worthy point to mention here is that since the source rate is generated higher than the TMT and the throughput at the destination node is much lower than the TMT, the overall packet loss ratio could be very high (>90% at 11 Mbps with RTS/CTS) in this set of simulations.

Now let us illustrate and discuss the simulation results shown in Figs. 5–8. For each scenario listed in Table 4, we have simulated the performance of a chain topology ad hoc network for both CSMA/CA and RTS/CTS mechanisms. The results for Scenario I are depicted in Figs. 5 and 6, and the corresponding results for Scenario II are shown in Figs. 7 and 8. In fact, the difference between these two scenarios, i.e., different distance between neigboring nodes, has also led to a spin-off result on chain topology throughput, as explained later in this subsection.

The first impression we get from these figures is that even though the one hop TMT varies greatly as the datarate changes, the difference between chain throughput among various datarates shrinks rapidly as the chain length grows. For example, when the chain length is 6 hops, the throughput for 11

[2]Of course, the nodes closer to the destination may not be saturated, but one cannot send higher bitrate at the source node. In other words, higher source rate would not result in a higher chain throughput at the destination.

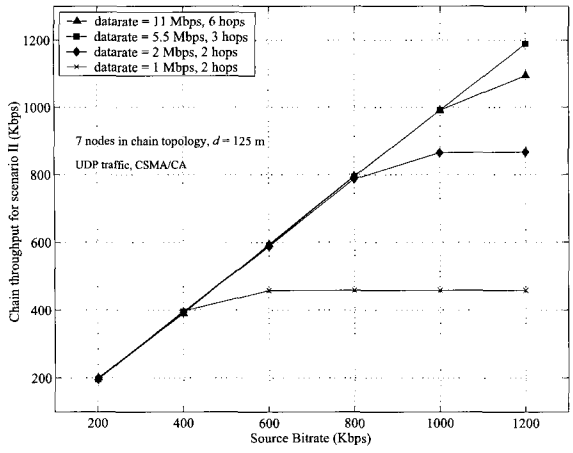


Fig. 9. Chain throughput for multihop ad hoc networks at different data rates with CSMA/CA (Scenario II). Moderate CBR/UDP traffic. The number of hops for data rate 11, 5.5, 2, or 1 Mbps is 6, 3, 2, or 2, respectively.

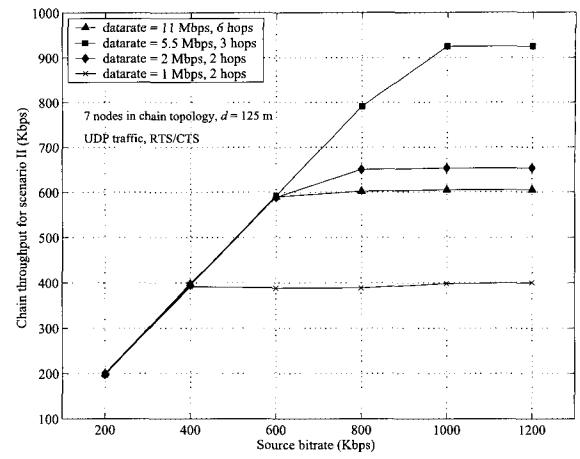


Fig. 10. Chain throughput for multihop ad hoc networks at different data rates with RTS/CTS (Scenario II). Moderate CBR/UDP traffic. The number of hops for data rate 11, 5.5, 2 or, 1 Mbps is 6, 3, 2, or 2, respectively.

Mbps datarate is at most twice as high as that for 1 Mbps, for all simulated cases. This is a remarkable contrast with the difference between the raw transmission datarates (11 Mbps versus 1 Mbps), and the one-hop TMT ($\sim$ 6 times difference between 11 and 1 Mbps in Table 1).

Let us examine the figures more carefully now. For CSMA/CA, Fig. 5 shows that there is a visible throughput difference among different datarates at quite long path. For another distance configuration shown in Fig. 7, there is almost no difference in chain throughput between datarates 5.5 and 11 Mbps when the chain length is larger than 6. Anyhow with CSMA/CA, the chain throughput for high datarates is still higher than that of low datarates. However, when RTS/CTS is enabled, the distinction disappears very soon. Figs. 6 and 8 illustrate that the chain throughput for all data rates is almost the same, once the chain length is 6 hops or more. To conclude, *there is almost no gain in applying high datarate in multihop ad hoc networks when the chain length is 6 hops or more.*

Moreover, this conclusion does not imply that using 11 Mbps is beneficial for chain length less than 6 either. Look at the results for Scenario II in Figs. 7 and 8 as an example. The throughput for 11 Mbps drops so sharply that 5.5 Mbps has achieved indeed higher throughput when chain length is of 2$\sim$6 hops. This is simply because that the path length at 5.5 Mbps is only one half of that at 11 Mbps in this case.

The above results show that the benefit of using high datarate diminishes as path length increases. This is because the overhead in 802.11 is comparatively heavier at higher datarate, and as path length grows, the overhead is incurred more and more times, resulting in a diminished gain from high datarate. With RTS/CTS, the per-hop overhead is even heavier. The chain throughput with RTS/CTS thus converges more tightly at long chain length, since this even-heavier per-hop overhead has to be repeated several times at multihop.

Here we would also like to present a spin-off result on chain throughput for *single datarate*, as an enhancement to the conclusion in [22]. Take 11 Mbps as an example, as shown in Figs. 5–6. Depending on which mechanism is used, the chain throughput achieved at node 12 is less than 1/10 or 1/20 of the one-hop TMT, for CSMA/CA or RTS/CTS, respectively (note that this conclusion is independent of which datarate is used). What we observe here is substantially lower than the result they reported. However, the reason for this result is simple: with shorter distance between neighboring nodes, more nodes take part in channel contention, since now more nodes are covered by the same interference range. More specifically with our distance configuration, only nodes which are 5- or 6-hops away from each other can transmit simultaneously. With RTS/CTS enabled, this effect is more serious since the CTS frames sent by the receiver can reach even further.

### *B. Performance at Moderate Traffic Load*

In this subsection, with a more realistic scheme, we continue to study the performance of the multihop networks, at moderate traffic loads. The distinction from the maximum throughput study above is that, with moderate traffic load, we are able to identify a range of network 'supportable' *source* bitrates that experiences high throughput, low delay and low packet loss in the network, for each datarate. To conduct this experiment, the source bitrate is set as 1200, 1000, 800, 400, or 200 Kbps respectively for the same packet length.

Having concluded from the above subsection that the benefit of using 11 Mbps disappears with path length of 6 hops, we continue the study on chain topology with only 7 nodes here. The number of hops between source and destination becomes 6, 3, 2, or 2 at 11, 5.5, 2, or 1 Mbps correspondingly. Scenario II in Table 4 is employed in this set of simulations.

#### B.1 Achievable Chain Throughput

Ideally, the network should be able to provide a quite linear throughput curve at moderate load. The problem is that as the chain length increases, the multihop network soon becomes saturated. Figs. 9 and 10 illustrate the chain throughput achieved at node 6, for CSMA/CA and RTS/CTS, respectively. Using the source bitrate as the horizontal axes, the figures show when the

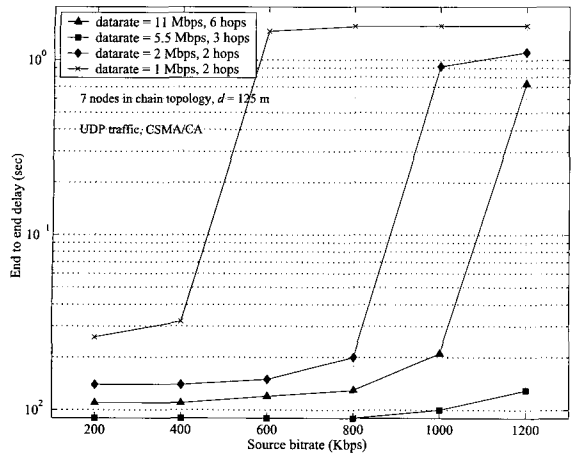


Fig. 11. End-to-end delay for multihop ad hoc networks at different data rates with CSMA/CA. Moderate CBR/UDP traffic. The number of hops for data rate 11, 5.5, 2, or 1 Mbps is 6, 3, 2, or 2, respectively.

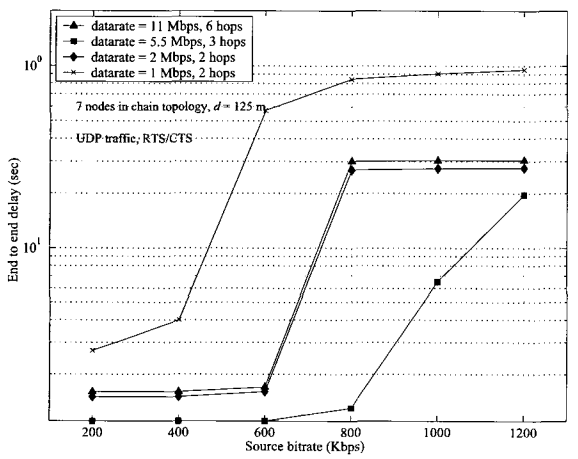


Fig. 12. End-to-end delay for multihop ad hoc networks at different data rates with RTS/CTS. Moderate CBR/UDP traffic. The number of hops for data rate 11, 5.5, 2, or 1 Mbps is 6, 3, 2, or 2, respectively.

network becomes saturated, at each datarate. 5.5 Mbps achieves the highest 'supportable' source rate, with both mechanisms. Interestingly with RTS/CTS, the supportable bitrate at 11 Mbps has decreased even below that of 2 Mbps. However, it is not very surprising if we notice that the path length at 2 Mbps is only one third of that at 11 Mbps. The 3-time TMT benefit by 11 versus 2 Mbps has been counteracted by the 3-time longer path.

### B.2 End-to-End Delay

Figs. 11 and 12 illustrate the ETE delay results with CSMA/CA and RTS/CTS, respectively, with a logarithmic vertical axis. Even though the one-hop delay is much shorter at 11 Mbps, the difference becomes smaller as the chain length increases. Once the channel becomes saturated, the ETE delays jump dramatically to hundreds of milliseconds, or even seconds, level for all datarates.

In summary, in this subsection we have investigated the performance of an 802.11b based multihop ad hoc network in chain topology, at relatively moderate network load. There are a few quite interesting observations in the context. Firstly, when the traffic load is very light (<400 Kbps), the source application can enjoy 'guaranteed' service for all concerned performance parameters (i.e., chain throughput, ETE delay and packet loss ratio) at any datarate. In this case, a sender would probably prefer to use datarates 1 or 2 Mbps to reduce the number of hops to destination, if the intrinsic transmission delay at low datarate is tolerable for the application. Secondly, for a medium traffic load (around 400–800 Kbps), the higher datarates achieve better performance than their lower datarate counterparts. However in this case, one would probably like to use 5.5 Mbps, not 11 Mbps, since it provides both 'guaranteed' performance and shorter number of hops. Finally, when the traffic load is comparatively heavy (>1000 or 1200 Kbps for RTS/CTS or CSMA/CA, respectively), there is no convincing performance at all, at any datarate. Why should we use high datarate even in this case? As a means to avoid network congestion, one would prefer to introduce rate control at the source node. However, that is outside the scope of this paper.

## V. NUMERICAL RESULTS WITH NODE MOBILITY

This section presents and discusses the simulation results based on a mesh topology with node mobility. To make a statistically more accurate observation on the performance of the concerned network, we generate a set of 10 diverse mobility patterns for each mobility configuration. Each configuration corresponds to an identical setting of average speed, pause time, etc. For instance, for the same average velocity of 5 m/s and pause time of 10 sec used in our simulations, the nodes move according to 10 different trajectories. The simulation results to be illustrated below are the average values from 10 mobility patterns.

We have mentioned earlier that the number of hops between source and destination nodes listed in Table 4 is only an 'ideal' value for stationary chain topology. In reality, this number, as well as the routing path, is decided by the routing protocol being used, and the routing protocol may choose more hops than the ideal number of hops. Therefore, it is of interest to investigate the number of hops at different datarates, especially when nodes are moving, since path length may vary from time to time due to mobility. In addition to the number of hops, we are also investigating other parameters, the average throughput, end-to-end delay and packet loss ratio in this section. Furthermore, we have run two sets of simulations, with CSMA/CA or RTS/CTS, for this scenario. However, we present only simulation results with CSMA/CA in this section.

### A. Average and Maximum Numbers of Hops

Table 5 lists the experienced average and maximum number of hops at each datarate, for homogeneous traffic pattern. Here, $N_{hops}^{ave}$ and $N_{hops}^{max}$ denote the average and the maximum numbers of hops, respectively.

As expected, the simulation results on the number of hops coincide with our intuitive impression from chain topology in Section III. That is, higher datarate leads to higher number of hops. Moreover, even though the average number of hops is

Table 5. Average and maximum number of hops at different datarates (Averaged from 4 pure CBR/UPD flows).

| | 11 Mbps | 5.5 Mbps | 2 Mbps | 1 Mbps |
|---|---|---|---|---|
| $N_{hops}^{ave}$ | 4.2 | 2.7 | 1.9 | 1.2 |
| $N_{hops}^{max}$ | 15.1 | 8.4 | 7.4 | 5.7 |
| $N_{neighbor}$ | 6.0 | 15.9 | 34.9 | 66.0 |

Table 6. Average throughput/goodput for UDP and TCP flows, in Kbps.

| Homogeneous | 11 Mbps | 5.5 Mbps | 2 Mbps | 1 Mbps |
|---|---|---|---|---|
| UDP | 133.9 | 180.0 | 149.3 | 123.5 |
| **Heterogeneous** | **11 Mbps** | **5.5 Mbps** | **2 Mbps** | **1 Mbps** |
| UDP | 102.3 | 137.3 | 100.7 | 66.7 |
| TCP | 372.8 | 522.6 | 390.0 | 267.0 |

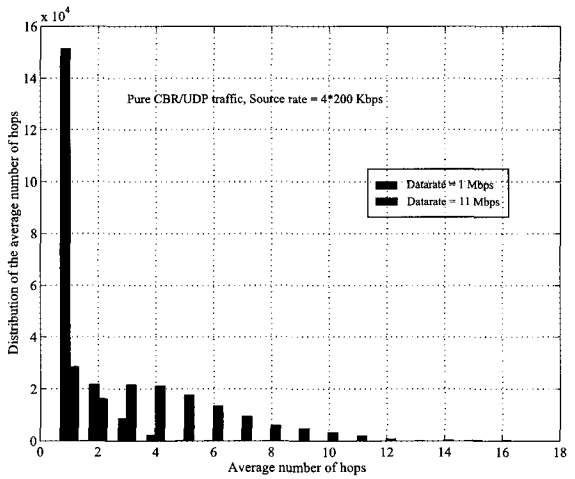


Fig. 13. Histogram showing the distribution of the number of hops at datarates 11 and 1 Mbps, for pure UDP traffic.

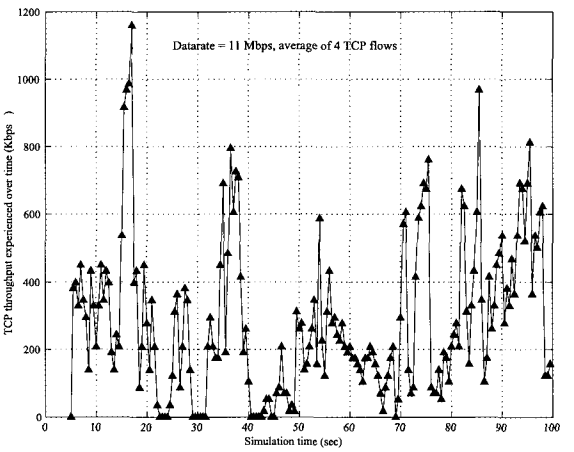


Fig. 14. Average TCP throughput over time, for heterogeneous traffic pattern. Datarate = 11 Mbps. TCP traffic starts at second 4.

quite low as shown in the table, some paths may be very long. As two extreme cases, Fig. 13 further illustrates the distributions of the number of hops at datarates 1 and 11 Mbps, respectively. At 1 Mbps, a majority of destinations are directly reachable by the source nodes. It is seldom in this case that a path would be longer than 4 hops. At 11 Mbps, on the other hand, many packets may need to transfer over multiple hops, even up to 15 hops. Although there is only a small minority of packets with very long paths, those 'misbehaved' packets deteriorate the overall performance significantly, e.g., to the average ETE delays as will be shown later.

Recall the 6-hop conclusion obtained from chain topology earlier and notice that the average number of hops at 11 Mbps is only 4.2 in this case. One might expect that 11 Mbps performs better than other datarates. However, as will be illustrated below, the benefit of using high datarate diminishes at even shorter path length when the mesh topology with node mobility is involved.

### B. Average Throughput

The simulation results on average throughput for both traffic patterns are tabulated in Table 6, where a successfully received packet may need from 1 to $N_{hops}^{max}$ hops to reach the destination.

As shown in the table, the achieved average throughput is really not satisfactory, for both traffic patterns. With pure UDP traffic, only 5.5 Mbps managed to provide 90% of the required bandwidth, and the throughput achieved at 11 Mbps is even lower than that at 2 Mbps. When heterogeneous traffic where 4 UDP and 4 TCP flows co-exist, however, 5.5 Mbps can only achieve about $2/3$ of the required bandwidth, while only half of the required bandwidth is obtained at 11 and 2 Mbps. 1 Mbps performs worst in both cases due to its intrinsic datarate limitation. In the heterogeneous case, the rest of the used bandwidth is absorbed TCP traffic.

The reason that TCP flows achieve higher throughput than UDP flows is due to TCP's capability to adjust its source rate according to network congestion status. Fig. 14 illustrates how TCP behaves against simulation time. Generally, TCP tries to send more packets when the network is less congested, and vice versa. There are also periods in which TCP traffic is fully stopped. This adaptivity gives TCP traffic high throughput and a very low packet loss, as will also be shown later.

In general, 5.5 Mbps performs best with node mobility, for both UDP and TCP traffic. This implies that, with the parameters settings used in this study, the tradeoff between the number of hops and chain throughput is optimally achieved at datarate 5.5 Mbps, for the studied 802.11b multihop network.

### C. End-to-End Delay

The average, minimum and maximal end-to-end delays simulated are tabulated in Table 7, denoted by $D_{ave}$, $D_{min}$, and $D_{max}$, respectively. We also list in the table the percentage of the successfully received packets that have ETE delays shorter than 250 ms, corresponding to the radio access bearer transfer delay for streaming traffic class defined in [23]. The end-to-end delays in the context include also accumulated queueing delays at all intermediate node(s).

The minimum delays represent the situation where the destination nodes are only one hop away from the source nodes, and the packets 'luckily' acquire the channel immediately when ready. However, even in the one-hop case, a packet may have

Table 7. End-to-end delays at different datarates.

| Homogeneous | 11 Mbps | 5.5 Mbps | 2 Mbps | 1 Mbps |
|---|---|---|---|---|
| $D_{ave}$ | 315 ms | 102 ms | 415 ms | 571 ms |
| $D_{min}$ | 1.4 ms | 1.2 ms | 2.4 ms | 4.5 ms |
| $D_{max}$ | 14.6 sec | 10.5 sec | 7.6 sec | 5.8 sec |
| $P_{D<250\text{ ms}}$ | 79% | 93% | 73% | 60% |
| Heterogeneous | 11 Mbps | 5.5 Mbps | 2 Mbps | 1 Mbps |
| $D^{ave}_{UDP}$ | 553.0 ms | 701.2 ms | 995.3 ms | 1795 ms |
| $P_{D<250\text{ ms}}$ | 63% | 51% | 43% | 21% |
| $D^{ave}_{TCP}$ | 90.6 ms | 78.7 ms | 85.0 ms | 139.0 ms |
| $P_{D<250\text{ ms}}$ | 93% | 99% | 95% | 89% |

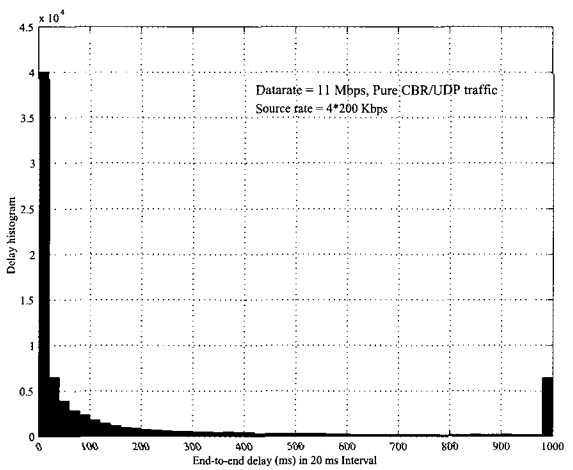


Fig. 15. Histogram showing the distribution of the end-to-end delay at 11 Mbps, for pure UDP traffic.

to wait in the queue at the source node before it is transmitted. Moreover, as illustrated from hop distribution, many packets have to transfer several hops before they reach the destination. In extreme cases, packets may have to wait up to several hundred of milliseconds or even seconds in the buffers at various nodes before they reach their destinations. This leads to a very long maximum delay in ranges of seconds, at all datarates. We have observed from the simulation results that, *compared with the backoff and transmission delays, the queueing delay dominates the end-to-end delay in multihop ad hoc networks.*

Furthermore, Fig. 15 illustrates the distribution of the ETE delay at 11 Mbps for homogeneous traffic. In this example, only 68% of the successful packets can enjoy short delay of $\leq$ 100 ms, while 8% packets have experienced long delay of over 1 second (the peak at the right-most point in the figure includes all packets with delay equal to or longer than 1 second).

### D. Packet Loss

Table 8 illustrates the simulated results on total packet loss ratio at different channel datarates, for both traffic patterns. As expected, higher packet loss happens to UDP traffic since the same amount of packets are generated at the source nodes, regardless of channel condition and network traffic load. With TCP traffic, however, the source nodes can adjust its bitrate accordingly, resulting in a very low TCP packet loss, at all datarates.

Table 8. End-to-end delays at different datarates.

| Homogeneous | 11 Mbps | 5.5 Mbps | 2 Mbps | 1 Mbps |
|---|---|---|---|---|
| UDP | 33% | 9% | 25% | 39% |
| Heterogeneous | 11 Mbps | 5.5 Mbps | 2 Mbps | 1 Mbps |
| UDP | 48% | 32% | 49% | 66% |
| TCP | 2.0% | 1.7% | 1.7% | 2.3% |

Table 9. Topology and routing information obtained by OLSR.

| Datarate (Mbps) | 54 | 36 | 18 | 11 | 6 | 1 |
|---|---|---|---|---|---|---|
| $Route_{est}$ | 14 | 95 | 99 | 99 | 99 | 99 |
| $Hop_{ave}$ | 2.7 | 5.3 | 3.2 | 2.0 | 1.5 | 1.2 |
| $Hop_{max}$ | 5.3 | 9.5 | 5.9 | 4.8 | 2.6 | 2 |
| $Neighbor_{ave}$ | 3.4 | 6.2 | 13.2 | 33.4 | 47.0 | 82.3 |

## VI. NUMERICAL RESULTS FOR 802.11G NETWORKS

In this section, we present briefly another set of simulation results which are based on 802.11b/g based multihop wireless networks. More detailed information about this scenario and numerical results can be found in [20].

Basically for this scenario, we generate 100 static nodes uniformly distributed in a square area of $800 \times 800$ m$^2$. 6 datarates are selected as the candidate datarates for our performance evaluation, which are 54, 36, 18, 11, 6, and 1 Mbps, with corresponding transmission ranges as 76, 130, 183, 304, 396, and 610 m, respectively, according the Cisco Aironet Card specification [24]. It is worthy mentioning that due to the consideration that the later proposed rate adaptation algorithm in Section VII-C requires network topology information, OLSR has been chosen as the routing protocol for this scenario. With its proactive feature, OLSR provides us with necessary network topology and neighbor connection information beforehand no matter there exists any data traffic or not in the studied network.

### A. Topology and Routing Information Using OLSR

We study network connectivity first in this scenario. With this perspective, the most important two performance observations are: 1) How many destinations can be reached by the routing protocol, among all nodes distributed in the area, at each datarate; and, 2) how long would the routing path be, on average and at maximal, in number of hops, at each datarate. The simulation results are summarized in Table 9, where $Route_{est}$ means the average number of routes established, $Hop_{ave}$ and $Hop_{max}$ indicate the average and maximum path lengths *for the established routes.* As a reference, the average number of neighbors at each datarate, $Neighbor_{ave}$, is also listed in the table.

Since there are totally 100 nodes in the network, the $Route_{est}$ value would be 99 if all other nodes are reachable. The simulation results in Table 9 show that only datarates equal to or lower than 18 Mbps can achieve full connectivity. At 36 Mbps, routes to around 5% nodes cannot be established, thus selecting 36 Mbps as the 'working' datarate would be 'risky' from the perspective of full connectivity. Not surprisingly, datarate 54 Mbps provides very poor connectivity and this counteracts greatly with its advantage of high per-link capacity.

Table 10. End-to-end delay and packet loss ratio for CBR/UDP traffic.

| Datarate (Mbps) | 54 | 36 | 18 | 11 | 6 | 1 |
|---|---|---|---|---|---|---|
| $D_{ave}^{ETE}$ (ms) | 1.2 | 5.6 | 6.6 | 37.9 | 72.1 | 299.0 |
| Loss ratio (%) | 95 | 5 | 0 | 0.7 | 2.3 | 29.8 |
| Throughput (Kbps) | 2 | 38 | 40 | 39.7 | 39.1 | 28.1 |

Table 11. End-to-end delay and packet loss ratio for CBR/UDP traffic.

| Datarate (Mbps) | 54 | 36 | 18 | 11 | 6 | 1 |
|---|---|---|---|---|---|---|
| Throughput (Kbps) | 1124 | 1016 | 1953 | 1742 | 1570 | 399 |
| $D_{ave}^{ETE}$ (ms) | 16.8 | 30.3 | 9.2 | 11.3 | 21.9 | 66.2 |
| Loss ratio | 20.3% | $< 0.1\%$ | 0 | 0 | 0 | 0 |

### *B. End-to-End Delay and Packet Loss for UDP Traffic*

Among the 100 nodes uniformly distributed within the area, 20 nodes are arbitrarily chosen as 10 source-destination pairs. To avoid packet loss earlier observed at heavy traffic load, only light traffic load is generated for CBR/UDP traffic in this simulation. This implies that most packets experience mainly MAC delay and transmission delay over multihops. More specifically in this case, the CBR traffic generated at each source node is 40 Kbps, where the packet length is 500 bytes.

The simulation results shown in Table 10 are the average values of 10 flows over 10 different topologies, where $D_{ave}^{ETE}$ means the average end-to-end delay in milliseconds.

The reason that 54 Mbps receives very poor throughput is quite clear: Lack of connectivity. In fact, we observed in simulation that 95% of the generated packets are lost and no-route-to-destination is the only reason for this packet drop. Only in few cases where the destination nodes are geographically quite close to the source nodes, the CBR packets can be successfully delivered, and the average delay for those packets is very low due to the intrinsic short per-link delay at 54 Mbps. Otherwise, the generated packets are simply lost, resulting in a very high packet loss at 54 Mbps. The reason that packet loss is also observed at the lowest datarates is that too many HELLO messages are generated by neighboring nodes especially at 1 Mbps when almost all other nodes (82 out of 99) are a node's one-hop neighbors.

### *C. Throughput, End-to-End Delay and Packet Loss for TCP Traffic*

Finally, we conduct a set of simulations for FTP/TCP traffic based on the same network configuration as for CBR traffic. The simulation results regarding average throughput, end-to-end delay and packet loss are listed in Table 11.

Because of TCP's rate adaptation and retransmission mechanisms, the packet loss ratio is almost zero once there exists a path between source and destination. However, at the highest two datarates, especially at 54 Mbps, some nodes are isolated and not reachable due to lack of neighbors. Once those nodes are selected as the source or destination nodes, all packets (a few packets) at the starting phase of the corresponding TCP flows are lost. The TCP connections are not established at all in these cases (note that the loss ratio of around 20% at 54 Mbps listed in the table is the average percentage of the unsuccessful *flows*, not packets).

The statistics on throughput and end-to-end delays listed in Table 11 are based on established flows. The end-to-end delays at different datarates are jointly decided by path length, queueing delay, per-link delay and traffic load. At 54 Mbps, many flows are not established. The total traffic is correspondingly moderate, resulting in a short queueing delay. A long route is the main 'contributor' for the end-to-end delay in this case. At 36 Mbps, almost all TCP flows are established. The queueing delay contributes significantly to the total delay at this datarate. At the lowest two datarates, there are also longer queueing delays partly due to more routing overhead mentioned earlier, in addition to TCP traffic. Of course, the intrinsic long per-link delay at lower datarates makes the end-to-end delay even longer in these cases.

## VII. PERFORMANCE ANALYSIS AND AUTOMATIC RATE SELECTION ALGORITHM

In the above three sections, we have demonstrated that the highest datarate(s) does(do) not lead to best performance in 802.11 based mutihop wireless networks. There are a number of reasons that can have impact on this behavior. For example, factors like channel condition, sensing range, protocol overhead, traffic characteristics etc may affect the performance of such multirate networks. However, we believe that increased path length and less connectivity, are among others, two major reasons for the performance degradation at high datarates. Therefore in the following subsections, we analyze end-to-end throughput and network connectivity in multirate wireless networks first, and then, based on our analytical results, propose an auto-rate selection algorithm for such networks.

### *A. Multihop End-to-End Throughput*

To make an approximation of the multihop throughput, we first calculate the transmitter separation distance, $S^{T-T}$, based an interference model [9], [10]. As depicted in Fig. 4, $S^{T-T}$ denotes the distance in hops between two immediate transmitters that can transmit simultaneously, and a smaller $S^{T-T}$ indicates a better spatial reuse.

Given the two-ray propagation model used in this study, the received signal strength at the receiver can be simply expressed as [25]

$$P_r = \frac{P_t G_t G_r h_t^2 h_r^2}{d^4} = \frac{C}{d^4} \tag{1}$$

where $d$ is the distance between the transmitter and the receiver, and $C$ represents a constant containing transmission power $P_t$, antenna gains $G_t$ and $G_r$, and the antenna heights of the transmitter and the receiver $h_t, h_r$.

First, consider the chain network in Fig. 4. The accumulated signals from other simultaneous transmitters, which are $H$ hops away from transmitter $T$, are interference to receiver $R$ and can be calculated as [12]

$$I_{rx}^R = \frac{C}{(H-1)^4 d^4} + \frac{C}{(H+1)^4 d^4} \tag{2}$$

Table 12. End-to-end delay and packet loss ratio for CBR/UDP traffic.

| Datarate | 11 Mbps | 5.5 Mbps | 2 Mbps | 1 Mbps |
|---|---|---|---|---|
| $\eta_{th}$ | 20.1 dB | 15.0 dB | 8.2 dB | 1.8 dB |
| $S_{1D}^{T-T}$ | 5.1 | 3.9 | 2.9 | 2.4 |
| $S_{2D}^{T-T}$ | 5.6 | 4.2 | 3.1 | 2.5 |

where interference from transmitters that are $mH$ ($m \geq 2$) hops away from the transmitting node is considered negligible and thus ignored. Symmetrically, the interference at $T$ when $R$ is transmitting an ACK to $T$ is $I_{rx}^{T} = I_{rx}^{R} = \frac{C}{(H-1)^4 d^4} + \frac{C}{(H+1)^4 d^4}$. Moreover, the background noise can be ignored, assuming an interference-limited environment. We can thus use signal-to-interference ratio (SIR) to approximate SINR, as follows

$$SIR^{1D} = \frac{P_r}{I_{rx}^{R} + I_{rx}^{T}} = \frac{(H^2-1)^4}{4(H^4+6H^2+1)}. \quad (3)$$

Similarly in the two dimensional case, the inference from the second tier and further away interfering nodes can be ignored. Thus by considering the first tier 6 nodes in a hexagonal area, the SIR in the 2-dimension (D) case can be approximated as [11]

$$SIR^{2D} = \frac{1}{\frac{2}{(X-1)^4} + \frac{1}{(X-\frac{1}{2})^4} + \frac{1}{X^4} + \frac{1}{(X+\frac{1}{2})^4} + \frac{1}{(X+1)^4}} \quad (4)$$

where $X = \frac{R_{cs}}{R_{tx}}$ is the ratio between the sensing range $R_{cs}$ and the transmission range $R_{tx}$. It corresponds to $S^{T-T}$ in the 2-D case and defines the minimum distance where simultaneous transmissions may occur.

Furthermore, to decode a packet correctly, we should have $SIR > \eta_{th}$, where $\eta_{th}$ is the required SIR threshold for each datarate. Now the transmitter separation distance $S^{T-T}$ can be obtained as $S^{T-T} = min(H)$ subject to $SIR > \eta_{th}$ and $Hd > R_{cs}$.

Finally, the end-to-end throughput for multihop networks can be approximately upper bounded by [10]

$$Throughput^{ETE} = \frac{Throughput^{per-hop}}{S^{T-T}} = \frac{TMT}{S^{T-T}}. \quad (5)$$

Numerically as an example, Table 12 lists the calculated $S^{T-T}$ for 802.11b, where the $\eta_{th}$ values are obtained based on Tab. 2 and the two-ray propagation model. Note the values for $S^{T-T}$ used here are for illustration purpose. In practice, these values should be integers.

The numerical results in Table 12 clearly indicate that the spatial reuse at 11 Mbps is much less than that of low datarates, leading to a degraded end-to-end throughput according to (5). As shown in the table, the throughput degradation at 11 Mbps is even worse with mesh topology since there are more nodes within the interference range in the 2-dimension case. This conclusion applies to other mutirate multihop 802.11 networks as well.

### B. $k$-Connectivity

Given the same node density, the number of one-hop neighbors for each node becomes fewer with shorter transmission range, making the network less connected. In the following, we first deduce a general formula for calculating the minimum node degree by assuming an ideal uniform node distribution, and then discuss its effect on average throughput.

Consider a homogeneous Poisson point problem in one dimension. A number of $n$ nodes where $n \gg 1$ are randomly *uniformly* positioned in an interval $[0, x_{max}]$. The probability that $k$ of $n$ nodes are placed in the interval $[x_1, x_2]$, where $0 \leq x_1 \leq x_2 \leq x_{max}$, is given by [26]

$$P(\mu = k) = \binom{n}{k} p^k (1-p)^{n-k} \quad (6)$$

where $\mu$ is a random variable denoting the number of nodes within the given interval, and $p$ is the probability that a node is placed within the interval $[x_1, x_2]$, as $p = \frac{x_2 - x_1}{x_{max}}$ in the one-dimension case.

With two dimensions, the problem becomes what is the probability that there are $k$ of $n$ nodes distributed within a certain area of $A_0$, given the total system area as $A$. Assume omnidirectional antenna with transmission range $r_0$ and a rectangular system area of $x_{max} \cdot y_{max}$. We have $A_0 = \pi r_0^2$ and $A = x_{max} \cdot y_{max}$. The probability that there is one node within the area of $A_0$ is simply $p = \frac{\pi r_0^2}{x_{max} \cdot y_{max}}$.

Analogous to the one dimension case, the probability that there are $k$ nodes distributed within $A_0$ can be obtained by substituting $p = \frac{\pi r_0^2}{x_{max} \cdot y_{max}}$ into (6). Therefore, the probability that each node has at least $k$ neighbors, i.e., the network has a minimum node degree $\mu_{min} \geq k$, or the network is $k$-connected, can be calculated by

$$\begin{aligned} P(\mu_{min} \geq k) &= 1 - \sum_{j=0}^{k} P(\mu = j) \quad (7) \\ &= 1 - \sum_{j=0}^{k} \binom{n}{j} (\frac{A_0}{A})^j (1 - \frac{A_0}{A})^{n-j}. \end{aligned}$$

Considering a wireless network in a rectangular area with $A = x_{max} \cdot y_{max}$ and each node has an omnidirectional antenna with transmission range $r$, the above expression can easily be used for calculating $k$-connectivity by substituting $A_0 = \pi r^2$ and $p = \frac{A_0}{A} = \frac{\pi r^2}{x_{max} \cdot y_{max}}$ into (7).

Numerically, Tables 13 and 14 list the calculated probabilities of $k$-connectivity at each datarate in our study for 802.11b ($k$ = 3, 6, 10, 15) and 802.11g ($k$ = 6), respectively. Note that the actual node degrees in our simulation with mobility would be biased due to the border effect and velocity instability problems in the random waypoint model [27], [28].

Furthermore, identifying the required minimum value of $k$ for a fully connected wireless network is not a trivial task. Early results showed that 6 or 8 as a 'magic number' for maximal throughput in a stationary and connected wireless network [29] [30]. Smaller [31] or larger number [32] has also been proposed later as the critical number under different circumstances, e.g., for stationary or mobile nodes. Another study [33] insisted that this value should be related to the total number of nodes inside the network and proposed to use $k = 5.1774 \log n$ for providing full connectivity. Through extensitive simulations, we found

Table 13. Probility of $k$-connectivity for at 802.11b, where $n = 100$, $x_{max} = y_{max} = 1200$ meters.

| Datarate | 11 Mbps | 5.5 Mbps | 2 Mbps | 1 Mbps |
|---|---|---|---|---|
| $P(\mu_{min} \geq 3)$ | 81.58% | 99.99% | 100% | 100% |
| $P(\mu_{min} \geq 6)$ | 32.54% | 99.76% | 100% | 100% |
| $P(\mu_{min} \geq 10)$ | 2.40% | 93.62% | 100% | 100% |
| $P(\mu_{min} \geq 15)$ | 0.01% | 53.16% | 99.99% | 100% |

Table 14. Probability of 6-connectivity for 802.11g where $A = 800 \times 800$ m$^2$ and $n = 100$.

| Datarate (Mbps) | 54 | 36 | 18 | 11 | 6 | 1 |
|---|---|---|---|---|---|---|
| $P(\mu_{min} \geq 6)$ (%) | 2.4 | 73.3 | 99.8 | 100 | 100 | 100 |

that $k = 6$ remains as a reasonable number for a static mesh network with uniform node distribution. Therefore, $k = 6$ is used in our rate adaptation algorithm which is decribed below.

Basically in a multihop network where a node has few neighbors, the probability that an end-to-end path can be established becomes very low. On the other hand, the UDP traffic is generated constantly at the application layer, regardless of network connectivity. As a consequence, more packets are discarded due to lack of paths or buffer overflow (packets are buffered in the queue when no path is found until the buffer is full). For example, during 100 second simulation period, one or more traffic flows may suffer from various length of duration with zero throughput due to no path to destinations, and those zero-throughput intervals contribute negatively to the average throughput, which is averaged over the whole simulation time.

### C. The Proposed Rate Adapation Algorithm

Assume that the number of nodes and the area of the network are known. The following procedures give a step-by-step summary of our rate selection algorithm, where $n$ is the total number of nodes, $A$ is the area of the network, $\omega_i (i = 1, 2, 3, \cdots, m)$ is the candidate datarates to be selected with $\omega_1$ corresponding to the highest datarate and $\omega_m$ corresponding to the lowest datarate.

`Step 1` Input $n$ and $A$. Let $i = 1$.

`Step 2` Calculate $P(\mu_{min} \geq 6)$ for $\omega_i$ according to (7).

`Step 3` If $P(\mu_{min} \geq 6) > 99\%$ for $\omega_i$, go to `Step 4`; Otherwise $i = i + 1$, go to `Step 2`.

`Step 4` $\omega_i$ is the selected datarate.

In other words, $\omega_i^{selected} = \omega_i^{highest}$ subject to $P(\mu_{min}^{\omega_i} \geq 6) > 99\%$. The benefit of employing the highest datarate with guaranteed connectivity is twofold. On the one hand, the selected high datarate provides the highest possible per-hop capacity, while ensuring a fully connected network. On the other hand, this selected high datarate can avoid extra protocol overhead due to responses to routing request broadcast, compared with other lower datarates which also provide full connectivity.

As an example, assuming $A = 800 \times 800$ m$^2$ and $n = 100$, the selected optimal datarate according to the above algorithm is 18 Mbps for a set of 802.11g datarates used in [20], which gives a probability of 6-connectivity as $P(\mu_{min}^{18M} \geq 6) = 99.8\%$. Correspondingly, for the set of datarates used in Sections IV and V, the selected optimal datarate is 5.5 Mbps by our algorithm. The numerical results illustrated earlier have shown that the selected datarate by the proposed rate adaptation algorithm overperforms the other datarates.

## VIII. RELATED WORK

The chain throughput of a multihop ad hoc network was concluded in [22] as $1/4 \sim 1/7$ of the one-hop throughput, and this conclusion is often cited by many other research papers. What we observe in this work shows that the chain throughput for single datarate could be substantially lower than $1/7$, to $1/10$ or even $1/20$ depending on whether RTS/CTS is used or not. We have further studied the chain throughput considering path length at different datarates.

In [5], the authors studied the relationship between transmission ranges and modulation schemes (datarates). They showed that, using a mobility scenario with only one UDP flow in a $1500 \times 300$ meter arena with 20 nodes, their proposed received-based rate adaptive (RBAR) algorithm outperforms its sender-based counterpart auto-rate fallback (ARF) used in [6], also in multihop networks. There are also other rate adaptation algorithms such as MiSer [34] and OAR [35]. However different from these algorithms, the proposed rate adaptation algorithm in this paper is based on our connectivity analysis with topology information support.

While testing their own implementation of the AODV protocol, the researchers in [36] observed that an unexpected large amount of packet loss occurred within certain specific geographic areas. These zones were termed as *communication gray zone* in [36], in which the next hops are shown to be reachable by routing messages, but the actual data packets cannot be received by the neighboring nodes. As also pointed out in [15], this phenomenon is caused by the different transmission ranges for control and data packets. Their observations reveal that the performance of many protocols may have to be re-evaluated since most previous work on this point were carried out by using ns2 default parameter settings. However, neither of them studied how multirange with multirate may affect the performance of a multihop ad hoc network.

The authors in another study in [37] have also noticed the problem in multihop ad hoc networks with different transmission ranges at different datarates. Their proposed route selection protocol prefers to select a high datarate link *when node density is sufficiently large*. They did not show, however, at how many number of hops the higher throughput using their algorithm is achieved . Our results in this paper demonstrate, on the contrary, that this benefit disappears when the path length is 6 even 4 hops.

The phenomenon of performance anomaly in 802.11b was studied in [19]. The authors observed that the throughput of all nodes transmitting at a higher datarate is degraded below the level of a lower datrate, when different datarates are used in the same WLAN. For this reason, we assume that all nodes along a path are using the same datarate in this study.

Finally, paper [26] deduced a closed-form expression for the probability of $k$-connectivity for an ad hoc network with uni-

form node distribution, assuming $x_2 - x_1 \ll x_{max}$ (the distance between any two nodes is much smaller than the dimension of the area). Their assumption led to a result that the probability of $k$-connectivity was very sensitive to transmission range. Our analysis in this paper, however, gives a general expression for this probability.

## IX. CONCLUSIONS AND FUTURE WORK

In this paper, we have demonstrated that higher transmission datarates do not necessarily provide better performance than lower datarates in multihop wireless networks. There are a number of conclusions that we can draw from this study.

First of all, based on the observation of different transmission ranges at various datarates and the frame structure analysis at the physical layer, we claim that there *always* exist *three* ranges in any frame transmission in 802.11, instead of *two* ranges as commonly understood in the literature, e.g., in [8], [16]. Secondly, we conclude that there is almost no gain by using the highest datarate in multihop wireless networks, when the path length reaches certain value. For instance in 802.11b networks, the benefit of using 11 Mbps disappears as the number of hops exceeds 6 (static networks) or 4 (with node mobility). Thirdly, we have studied the cons and pros of transmitting at a high datarate with shorter per-hop distance and longer path, or vice versa. A tradeoff must be found between network connectivity and end-to-end network performance when selecting the most appropriate datarate. Fourthly, based on our analysis on network connectivity for multirate networks, an auto-rate adaptation algorithm has been proposed.

Finally as our future work, the proposed auto-rate adaptation is to be further studied and implemented in a Linux based test bed, e.g., as a plug-in of the OLSR implementation OLSRD [38].

## ACKNOWLEDGMENT

This work is partly supported by the Research Council of Norway (NFR) through the FUCS project and partly supported by the European Commission through the ADHOCSYS project (IST-2004-026548). We would also like to thank Prof. Tracy Camp from Colorado School of Mines for providing us with their stationary random waypoint mobility model for our simulation.

## REFERENCES

[1] IEEE Computer Society, "Local and metropolitan area networks: Wireless LAN medium access control (MAC) and physical (PHY) specifications," IEEE std 802.11, 1999 Ed., 1999.

[2] IEEE Computer Society, "Supplement to part 11: Wireless LAN medium access control (MAC) and physical (PHY) specifications: high-speed physical layer extensions in the 2.4 GHz band," IEEE std 802.11b, 1999 Ed., 2000.

[3] IEEE Computer Society, "Supplement to part 11: Wireless LAN medium access control (MAC) and physical (PHY) specifications, amendment 4: Higher data rate extension in the 2.4 GHz band," IEEE std 802.11g, 2003 Ed., 2003.

[4] IEEE Computer Society, "Supplement to part 11: Wireless LAN medium access control (MAC) and physical (PHY) specifications: enhancements for higher throughput," IEEE P802.11n$^{TM}$/D2.0, Mar. 2007.

[5] G. Holland, N. Vaidya, and P. Bahl, "A rate-adaptive MAC protocol for multi-hop wireless networks," in *Proc. ACM MobiCom*, Rome, Italy, July 2001.

[6] A. Kamerman and L. Monteban, "WaveLAN-II: A high-performance wireless LAN for the unlicensed band," *Bell Labs Tech. J.*, pp.118–133, July 1997.

[7] J. P. Pavon and S. Choi, "Link adaptation strategy for IEEE 802.11 WLAN via received signal strength measurement," in *Proc. IEEE ICC*, Anchorage, USA, May 2003.

[8] E-S. Jung and N.H. Vaidya, "A power control MAC protocol for ad hoc networks," in *Proc. ACM MobiCom*, Atlanta, USA, Sept. 2002.

[9] X. Guo, S. Roy, and W. S. Conner, "Spatial reuse in wireless ad-hoc networks," in *Proc. IEEE VTC Fall*, Florida, USA, Oct. 2003.

[10] J. Zhu, X. Guo, L. L. Yang, W. S. Conner, S. Roy, and M. M. Hazra, "Adaptive physical carrier sensing to maximize spatial reuse in 802.11 mesh networks," *Wireless Commun. Mobile Computing*, vol. 4. no. 8, pp. 933–946, Nov. 2004.

[11] X. Yang and N. Vaidya, "On the physical carrier sense in wireless ad hoc networks," in *Proc. IEEE INFOCOM*, Miami, USA, Mar. 2005.

[12] F. Y. Li and Ø. Kure, "Optimal physical carrier sense range in multirate wireless ad hoc networks: Analytical versus realistic," in *Proc. European Wireless EW*, Nicosia, Cyprus, Apr. 2005.

[13] J. Jun, P. Peddabachagari, and M. Sichitiu, "Theoretical maximum throughput of IEEE 802.11 and its applications," in *Proc. Int. Symp. on Network, Computing and Applications (NCA)*, Cambridg, MA, USA, Apr. 2003.

[14] ORiNOCO Classic Gold PC Card, [Online]. Available: http://www.proxim.com/

[15] G. Anastasi, E. Borgia, M. Conti, and E. Gregori, "IEEE 802.11 ad hoc networks: Performance measurements," in *Proc. Workshop on Mobile and Wireless Networks (MWN)*, Rhode Island, USA, May 2003.

[16] The Network Simulator - ns-2, [Online]. Available: http://www.isi.edu/nsnam/ns/

[17] C. E. Perkins, E. M. Royer, and S. Das, "Ad hoc on-demand distance vector (AODV) routing," *RFC 3561, IETF*, July 2003.

[18] T. Clausen and P. Jacquet, "Optimized link state routing protocol (OLSR)," *RFC 3626, IETF*, Oct. 2003.

[19] M. Heusse, F. Rousseau, G. Berger-Sabbatel, and A. Duda, "Performance anomaly of IEEE 802.11," in *Proc. IEEE INFOCOM*, San Francisco, USA, 2003.

[20] F. Y. Li, E. Winjum, and P. Spilling, "Connectivity-aware rate adaptation for 802.11 multirate ad hoc networking," in *Proc. 19th International Teletraffic Congress (ITC)*, Beijing, China, Sept. 2005.

[21] W. Navidi and T. Camp, "Stationary distributions for the random waypoint mobility model," *IEEE Trans. Mobile Computing*, vol. 3, no. 1, pp. 99–108, Jan. 2004.

[22] J. Li, C. Blake, D.S.J. De Couto, H.I. Lee ,and R. Morris, "Capacity of ad hoc wireless networks," in *Proc. IEEE MobiCom*, Rome, Italy, July 2001.

[23] 3GPP TS23.107v6.1.0, "Quality of Service (QoS) concept and architecture," Mar. 2004, [Online]. Available: http://www.3gpp.org

[24] Cisco, "Aironet 802.11a/b/g wireless LAN client adapters CB21AG and P121AG installation and configuration guide: Appendix A," [Online]. Available: http://www.cisco.com

[25] T. S. Rappaport, *Wireless Communications, Principles and Practices*, 2nd Ed. New Jersey: Prentics-Hall, Inc., 2002.

[26] C. Bettstetter, "On the minimum node degree and connectivity of a wireless multihop network," in *Proc. ACM MobiHoc*, Lausanne, Switzerland, June 2002.

[27] C. Bettstetter, "Mobility modeling in wireless networks: Categorization, smooth movement, and border effects," *ACM MC2R*, vol. 5, no. 3, pp. 535–547, 2001.

[28] J. Yoon, M. Liu, and B. Noble, "Random waypoint considered harmful," in *Proc. IEEE INFOCOM*, San Francisco, USA, Mar. 2003.

[29] L. Kleinrock and J. Silvester, "Optimum transmission radii for packet radio networks or why six is a magic number," in *Proc. IEEE National Telecommunications Conf.*, Dec. 1978.

[30] H. Takagi and L. Kleinrock, "Optimal transmission ranges for randomly distributed packet radio terminals," *IEEE Trans. Commun.*, vol. 32, no. 3, pp. 246–257, 1984.

[31] G. Ferrari and O. K. Tonguz, "Minimum number of neighbors for fully connected uniform ad hoc wireless networks," in *Proc. IEEE ICC*, Paris, France, June 2004.

[32] E. M. Royer, P. M. Melliiar-Smith, and L. E. Moser, "An analysis of the optimum node density for ad hoc mobile networks," in *Proc. IEEE ICC*, Helsinki, Finland, May 2001.

[33] F. Xue and P. R. Kumar, "The number of neighbors needed for connectivity of wireless networks," *Wireless Networks*, vol. 41, no.2, pp. 169–181, 2004, Kluwer.

[34] Qiao, S. Choi, A. Jain, and K. S. Shin, "MiSer: An optimal low-energy transmission strategy for IEEE 802.11a/h," in *Proc. ACM MobiCom*, San Diego, USA, Sept. 2003.
[35] B. Sadeghi, V. Kanodia, A. Sabharwal, and E. Knightly, "OAR: An opportunistic auto-rate media access protocol for ad hoc networks," in *Proc. ACM MobiCom*, Altanta, USA, Sept. 2002.
[36] H. Lundgren, E. Nordström, and C. Tschudin, "Coping with communication gray zones in IEEE 802.11b based ad hoc networks," in *Proc. Int. Workshop on Wireless Mobile Multimedia (WoWMoM)*, Atlanta, USA, Sept. 2002.
[37] B. Awerbuch, D. Holmer, and H. Rubens, "High throughput route selection in multi-rate ad hoc wireless networks," in *Proc. First Working Conf. on Wireless On-demand Network Systems (WONS)*, Madonna di Campiglio, Italy, Jan. 2004.
[38] [Online]. Available: http://www.olsr.org

**Frank Y. Li** holds a Ph.D. degree from the Department of Telematics, Norwegian University of Science and Technology (NTNU). He works as a senior researcher at UniK - University Graduate Center, University of Oslo before joining the Department of Information and Communication Technology, University of Agder as an associate professor in August 2007. His research interest includes 3G and beyond mobile systems and wireless networks, mesh and ad hoc networks; QoS, resource management, and traffic engineering in wired and wireless IP-based networks; analysis, simulation, and performance evaluation of communication protocols and networks.

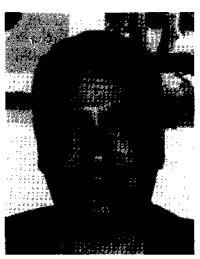

**Andreas Hafslund** has worked as a research engineer within mobile networking. He worked on routing, security, QoS and multicast issues, especially related to military tactical networks. Currently he is working for Telenor in Norway, as a product manager for IP networks. His research interests include IP networking issues for 3G and beyond mobile systems, especially related to routing, security, and multicast.

**Mariann Hauge** received her M.S. in Electrical Engineering from the University of California, Santa Barbara in 1994 and her Ph.D. from the Department of Informatics, University of Oslo in 2007. She curently holds a research scientist position at the Norwegian Defence Research Establishment (FFI). Her current research interest includes multicast and QoS in mobile networks.

**Paal Engelstad** holds a Ph.D. degree from the Department of Informaticts, University of Oslo (UiO). He is employed as a senior research scientist at Telenor Research and Innovation and as an associate professor II at UiO and the University Graduate Center at Kjeller (UniK). His current research interests include functional and performance analysis of networks and protocols by simulations, implementations and analytical models, especially related to mobility and IP access in wired and wireless networks, QoS, mesh, and ad hoc networks and the 802.11 WLAN MAC.

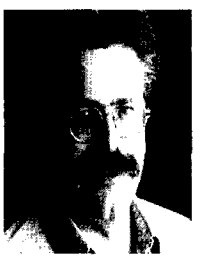

**Øivind Kure** is a professor at the Center for Quantifiable Quality of Service in Communication Systems and the Department of Telematics, Norwegian University of Science and Technology, Trondheim. He got his Ph.D. from the University of California, Berkeley in 1988. His current research interest includes various aspects of QoS, performance analysis, multicast protocols, and ad hoc networks.

**Pål Spilling** obtained his Ph.D. from the University of Utrecht, The Netherlands in 1968 in experimental low-energy neutron physics. Subsequently, he joined the nuclear physics group at the Technical University in Eindhoven, The Netherlands. In January 1972, he started to work for the Norwegian Defence Research Establishment (FFI) at Kjeller, and from end 1974 he got involved with the ARPA-funded research program in packet switching and Internet technology. He was in 1979/80 a visiting scientist with SRI International in Menlo Park, California, where he worked on the Packet Radio program. He joined the Research Department of the Norwegian Telecommunications Administration (NTA-RD) in August 1982. Subsequently, he established the first Internet outside USA, interconnected with the US internet. At NTA-RD he worked with communications security and the combination of Internet technology and fiber-optic transmission network. In 1993, he became a professor at the Department of Informatics, University of Oslo and UniK - University Graduate Center at Kjeller.